

Inner-shell alignment by Compton scattering

Friedhelm Bell and Hans Böckl

*Sektion Physik, Universität München, Am Coulombwall 1,
D-8046 Garching, Federal Republic of Germany*

(Received 22 October 1984)

The alignment of the $2p$ state by Compton scattering is investigated. Here, Compton scattering is understood as the inelastic scattering of large-momentum photons, electrons, or ions. At the peak position of the $2p$ Compton profile the alignment parameter A_{20} has its maximum possible value, $+0.5$.

If a projectile with large momentum \mathbf{p}_1 is inelastically scattered by a bound atomic electron, the energy distribution of either the projectile or the ejected electron reflects in essence what is called a Compton profile (CP). Up to now, measurements of this type have been made for incident photons (the usual Compton effect), electrons,^{1,2} and ions.³ It is the aim of this paper to show that strong alignment of the atomic state results from this kind of scattering. For a momentum transfer q which is large compared to the average intrinsic momentum $p_{0r} = Z/2$ of the atomic electron, it is easy to show that the doubly differential scattering cross section factorizes (atomic units are used):

$$\frac{d^2\sigma}{dE d\Omega} = \frac{1}{\nu} \left(\frac{d\sigma}{d\Omega} \right) J(p_z) \quad (1)$$

with

$$J(p_z) = \nu \int d^3\mathbf{p} |\psi(\mathbf{p})|^2 \delta(E - f(\mathbf{p}))$$

Within this so-called impulse approximation, $J(p_z)$ is the Compton profile, E the energy loss of the projectile, $\psi(\mathbf{p})$ the wave function of the bound electron, and Z the atomic number of the target atom. $(d\sigma/d\Omega)$ is the relevant scattering cross section, i.e., the Rutherford cross section in the case of electrons and ions and the Thomson cross section in the case of photons. The coefficient $\nu = dE/dp_z$ and the function $f(\mathbf{p})$ are determined by kinematics. For measurements of the projectile's energy loss (photons, elec-

trons) $\nu = q$ and $f(\mathbf{p}) = \mathbf{p} \cdot \mathbf{q} + q^2/2$, where

$$q = (p_1^2 + p_1'^2 - 2p_1 p_1' \cos\theta)^{1/2}$$

is the momentum transfer, θ the scattering angle, and p_1' the projectile momentum after the interaction. For incident ions and the measurement of the energy distribution of the ejected electron $\nu = 2v$ and $f(\mathbf{p}) = \mathbf{v}(\mathbf{p}_e - \mathbf{p})$ holds. \mathbf{v} is the projectile velocity and \mathbf{p}_e the electron momentum (i.e., $E_e = 0.5p_e^2$). Here, we are interested in the alignment of the initial atomic state, i.e., in the Compton profiles of the magnetic substates $2p_0$ and $2p_1$. For hydrogenic wave functions one obtains (per electron)⁴

$$J_{2p_0}(x) = \frac{2^8 x^2}{5\pi Z(1+x^2)^5}, \quad J_{2p_1}(x) = \frac{2^5}{5\pi Z(1+x^2)^4} \quad (2)$$

$$3J_{2p} = J_{2p_0} + 2J_{2p_1}$$

with $x = p_z/p_{0r}$. Here, $p_z = q/2 - E/q$ holds for electrons and photons and $p_z = p_e \cos\theta_e - E/v$ for ions. Figures 1(a)–1(c) show a comparison of the double differential cross section for a $2p_0$ initial state between an exact first Born approximation (solid curves) and the impulse approximation of Eq. (1) (broken curves). The figures hold for incident photons (a), electrons (b), and protons (c). The agreement is fairly good. In each figure caption $\kappa = q/p_{0r}$ is indicated. Since this ratio is about the same for all three processes, one expects nearly the same validity of the impulse approximation. An inspection of the matrix element

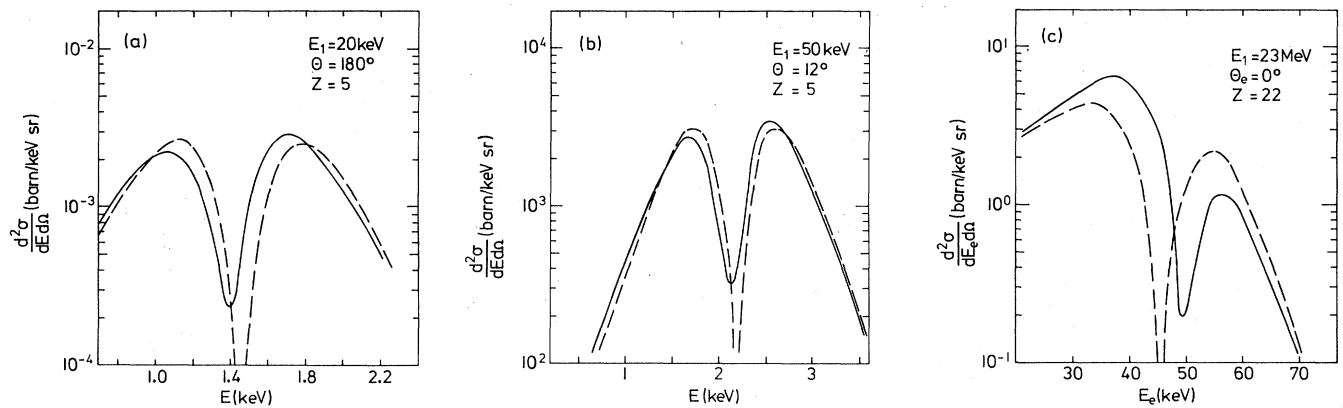


FIG 1. Comparison between the first Born approximation (solid curves) and the impulse approximation (broken curves) for a $2p_0$ initial state. E_1 is the projectile energy, θ the scattering angle (θ_e the electron emission angle in case of incident ions), and E the energy loss (E_e the electron's kinetic energy in case of ions). (a) incident photons, $\kappa = 4.3$; (b) incident electrons (see Ref. 9), $\kappa = 5.0$; (c) incident protons, $\kappa = 5.4$.

reveals that for $\kappa \gg 4\pi$ the Born and impulse approximation become identical. The Born approximation of Fig. 1(a) has been taken from Ref. 5, where it has been claimed erroneously that the impulse approximation does not reproduce the double peak structure of the Born approximation. The minimum of the cross section occurs at $p_z=0$ where the corresponding CP has a node. Such an inversion of the usual peak structure of a CP at $p_z=0$ occurs for every magnetic substate with hydrogenic quantum numbers $l+m = \text{odd}$.⁶ From Eq. (2) the component A_{20} of the alignment tensor follows:⁷

$$A_{20} = (J_{2p_1} - J_{2p_0})/3J_{2p} = (1 - 7x^2)/(2 + 10x^2). \quad (3)$$

Thus, if the Compton-scattered particle is measured in coincidence with an x-ray or an Auger electron, which are both characteristic for the $2p$ hole, an anisotropic emission intensity I follows. In the case of x-ray emission an intensity I is predicted:⁷

$$I(x, \phi) = \frac{I_0}{4\pi} [1 + \alpha_2 A_{20} P_2(\cos\phi)] \quad (4)$$

(Shell-specific Compton scattering by coincidence measurements is a well-established technique; see Ref. 8.) In Eq. (4), ϕ is the angle between the quantization axis and the x-ray detector. Inspection of the δ function in Eq. (1) reveals that the quantization axis is parallel to \mathbf{q} for photons and parallel to \mathbf{v} for ions. The coefficient I_0 is proportional to the $2p$ CP. Figure 2 shows $I(x)$ for $\phi = 90^\circ$ and the magic angle $\phi = 54.7^\circ$. In the latter case, I reflects the undisturbed $2p$ Compton profile. Interestingly, the curve for $\phi = 90^\circ$ demonstrates the effect of peak inversion. The curves have been calculated for an x-ray transition parameter $\alpha_2 = 0.5$, which corresponds to an L_I line. The effect of Coster-Kronig transitions which admixture electron-hole concentrations from nonaligned states prior to the x-ray transition is neglected. This would slightly reduce the influence of alignment, but would not destroy the effect

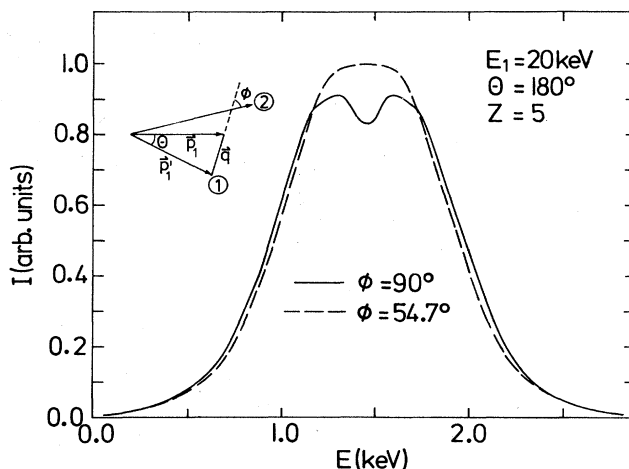


FIG. 2. The Compton profile of a $2p$ initial state, coincident with an L_I photon. Solid curve: $\phi = 90^\circ$; broken curve: $\phi = 54.7^\circ$. The inset shows the positions of the Compton detector 1 and the x-ray detector 2.

of inversion in Fig. 2. Thus, measurements of this kind are sensitive to CP's of magnetic substates.

Figures 1(a) and 1(b) have been calculated for $Z = 5$, for which an experiment of the kind described is impossible (there are no L_I lines). The reason is that the first Born approximation in Fig. 1(a) is taken from Ref. 5 and the authors did not calculate for larger Z values, and Fig. 1(b) shall demonstrate the large difference in absolute cross sections between photon and electron scattering. Nevertheless, Figs. 1(a) and 1(b) reveal the general behavior of the cross section; within the impulse approximation the target nuclear charge Z enters only in p_0 , (and not in $d\sigma/d\Omega$). Thus, extension to other Z values can easily be achieved. Especially, the strong correlation effect of Fig. 2 remains unchanged.

¹B. Williams, *Compton Scattering* (McGraw-Hill, New York, 1977).

²A. D. Barlas, W. H. E. Rueckner, and H. F. Wellenstein, *J. Phys. B* **11**, 3381 (1978).

³F. Bell and H. Böckl, *Nucl. Instrum Methods Phys. Res. Sect. B* **2**, 311 (1984).

⁴R. Spies, H. Böckl, F. Bell, and D. H. Jakubassa-Amundsen, *J. Phys. B* **17**, 2841 (1984).

⁵B. J. Bloch and L. B. Mendelsohn, *Phys. Rev. A* **9**, 129 (1974).

⁶H. Böckl, R. Spies, F. Bell, and D. H. Jakubassa-Amundsen, *Phys. Rev. A* **29**, 983 (1984).

⁷E. G. Berezhko and N. M. Kabachnik, *J. Phys. B* **10**, 2467 (1977).

⁸P. P. Kane and P. N. Baba Prasad, *Phys. Rev. A* **15**, 1976 (1977).

⁹P. Swan, *Proc. R. Soc. London, Ser. A* **68**, 1157 (1955).